

^{14}N Fourier Transform Nuclear Quadrupole Resonance. Instrumentation: Measurements on Cyanuric Chloride*

Roberto Ambrosetti, Claudia Forte, and Domenico Ricci

Istituto di Chimica Quantistica ed Energetica Molecolare del CNR, Pisa, Italy

Z. Naturforsch. **47a**, 421–429 (1992); received August 23, 1991

A Matec pulsed instrument, already equipped with a laboratory-built data system, has been considerably improved by adding new capabilities, such as versatile pulse sequence programming. Among other things, this allows automated T_1 relaxation measurements. The instrument has been employed to record the ^{14}N NQR FT spectrum of cyanuric chloride and measure its T_1 relaxation time from 77 K to the melting point at 418 K. The four-line ^{14}N spectrum indicates the presence of two chemically inequivalent sites. The intensity ratio of the lines identifies the site pertaining to a couple of symmetry-related ^{14}N nuclei. The lines smoothly decrease in frequency up to the melting point, where they remain narrow and almost equally spaced. Considering previous results at 4.2 K, this indicates that a single phase is stable over the entire accessible temperature range. The relaxation time T_1 decreases smoothly with increasing temperature, with a T^{-2} law, from nearly 180 s at 77 K to about 1 s near the melting point, where a precipitous decrease starts. The high T_1 values found are consistent with the lack of nuclei having high magnetic moment.

Introduction

Cyanuric chloride has been the object of many investigations through the history of NQR research. This is certainly due to its interesting structure and properties. It has a highly symmetric structure and contains a hetero ring having marked aromatic properties. It contains two types of widely studied quadrupolar nuclei but no other nuclei, such as ^1H or ^{19}F , having high magnetic moment. It also has unusual chemical properties, such as the ability to undergo stepwise nucleophilic substitution of Cl atoms under mild conditions [1], which attests a peculiar electronic structure.

The first observation of a ^{35}Cl NQR spectrum dates back to 1957 [2]. A two-line spectrum was found, consisting of two narrow, very closely spaced lines with an approximately 2:1 amplitude ratio. One year thereafter, cyanuric chloride has been the object of two of the very first single-crystal Zeeman studies [3], whose findings were consistent with the partial structure data found shortly before by X-ray diffraction [4]. It was also the object of one of the first powder Zeeman pattern investigations [5].

A two line ^{14}N spectrum was also measured in an early study [6]. Today this spectrum is known to be incomplete. In fact, in cyanuric chloride the three nitrogen atoms, as well as the three chlorine atoms, are found on two different kinds of sites resulting in a two line chlorine spectrum ($I = 3/2$ yields one line per site) and a four line nitrogen spectrum ($I = 1$ yields two lines, ν^+ and ν^- , per site), the corresponding intensities being in a 2:1 ratio.

Pulsed and Fourier Transform methods were soon employed as they became available. Thus cyanuric chloride has been the object of early ^{35}Cl FT investigations [7]. One of the few two-dimensional NQR FT experiments so far performed has been carried out on it [8]: the two chemically equivalent ^{35}Cl sites were resolved by a small Zeeman field, which was applied over a time interval whose length yielded the second "dimension". A variable-temperature study on ^{14}N has been performed by pulsed methods [9] from 77 K to about 380 K, but it again failed to detect the full 4-line spectrum. The complete ^{14}N spectrum, obtained by FT methods at room temperature, was presented in a poster from this Laboratory at the Darmstadt NQR Symposium, where the detection of the full set of lines at liquid He temperature was also announced and later published [10].

Cyanuric chloride thus appears as a standard reference compound for the application of new NQR techniques. We turned to it for just the same reason. In fact we intended to check the ability of our new NQR data

* Presented at the XIth International Symposium on Nuclear Quadrupole Resonance Spectroscopy, London, U.K., July 15–19, 1991.

Reprint requests to Dr. R. Ambrosetti, Istituto di Chimica Quantistica ed Energetica Molecolare del CNR, Via Risorgimento, 35, I-56126 Pisa, Italy.

0932-0784 / 92 / 0100-0421 \$ 01.30/0. – Please order a reprint rather than making your own copy.



Dieses Werk wurde im Jahr 2013 vom Verlag Zeitschrift für Naturforschung in Zusammenarbeit mit der Max-Planck-Gesellschaft zur Förderung der Wissenschaften e.V. digitalisiert und unter folgender Lizenz veröffentlicht: Creative Commons Namensnennung-Keine Bearbeitung 3.0 Deutschland Lizenz.

Zum 01.01.2015 ist eine Anpassung der Lizenzbedingungen (Entfall der Creative Commons Lizenzbedingung „Keine Bearbeitung“) beabsichtigt, um eine Nachnutzung auch im Rahmen zukünftiger wissenschaftlicher Nutzungsformen zu ermöglichen.

This work has been digitalized and published in 2013 by Verlag Zeitschrift für Naturforschung in cooperation with the Max Planck Society for the Advancement of Science under a Creative Commons Attribution-NoDerivs 3.0 Germany License.

On 01.01.2015 it is planned to change the License Conditions (the removal of the Creative Commons License condition "no derivative works"). This is to allow reuse in the area of future scientific usage.

system [11] to cope with wide spectra containing multiple, narrow lines. We also wanted to add to it new capabilities specifically required for relaxation time measurements.

So we report here both on such instrumental developments and on NQR results of intrinsic interest.

Experimental

Sample Preparation

Cyanuric chloride (FLUKA purum) was used without further purification, as manipulations would create the possibility of partial hydrolysis, thus introducing in the crystal lattice a number of ^1H nuclei, which could affect the T_1 measurements. In fact cyanuric chloride emits dense fumes in moist air. The fine crystalline powder was transferred to a glass vial under dry nitrogen in a glove box, and all subsequent manipulations prior to sealing the vial were carried under nitrogen.

Two samples were prepared, both about 6 ml in volume. The first was obtained by melting cautiously the powder sample in the glass vial, then letting it resolidify and cool slowly within a polyurethane block.

The second was obtained by simply vibrating the vial: this compacted the sample to some extent, but considerably less (perhaps a factor of 2) than the melted one. The second sample was used to check the ratio of the amplitudes of the lines and of the relaxation times at some temperatures, since the melted sample could have developed anisotropies in the solidification process. Since no signs of anisotropy were detected, the melted sample, which gave a considerably stronger signal, was used for all measurements.

Instrumentation

The NQR instrument comprises [12] a 5100 Gating Modulator, a 515 plug-in and a 615 Receiver, all by Matec. The rf source is an HP 3325 A synthesizer.

The cryostat is also as described. It employs electric heating and is cooled by direct injection of droplets of liquid nitrogen, under control of a laboratory-built thermostat. It was modified to extend its high-temperature limit. Polytetrafluoroethylene is now used for all non-metallic parts, including the insulator of the short rf cable connecting the coil to the rest of the instrument. A miniaturized (1 by 5 mm) Pt resistor is the

thermometer. It is mounted just below the sample, screened by a small brass tube grounded at the electrically "cool" side of the coil. This allows reliable temperature measurements without any rf disturbance.

Data Acquisition and Processing

The associated data system has been described in detail [11]. It consists essentially of a specially designed data interface, puggable in any MS-DOS PC having an AT-type slot. The system has a maximum data-acquisition rate of 250 kHz (500 kHz interlaced) including 32-bit real-time time averaging, and the A/D converter has 12-bit resolution. Most time-related tasks are performed by programmable timers on the interface itself.

Assembly-language subroutines give access to all hardware functions through simple CALL statements in a QuickBASIC main program whose main functions are: interpretation of user commands; acquisition and storage of data; one-line display and non-linear least squares (NLLSQ) fit of either the FID or its FT spectrum. Such tasks can be performed during acquisition itself.

For the present measurements we added features allowing essentially unlimited pulse programming. The hardware is now capable of issuing a pulse whose duration and repetition rate are software programmable. A few μs is enough to reprogram the next pulse. This time is almost always available between the end of the acquisition (if any) following the pulse and the start of the next pulse. This process can be repeated endlessly. Maximum pulse separation is about 5 months, with 100 ns resolution maintained throughout.

Using pulse programming, the QuickBASIC main program allows automatic, unattended T_1 measurements. The operator only chooses, on the first acquired data, the spectral lines on which T_1 is to be measured. The effect of long-term drift, important for the measurement of long T_1 's, is counteracted by "scrambling" the sequence of pulse separations. A follow-up capability of the spectral lines is also included in the program, which can even record the "thermal history" of the sample or any other time-dependent event. To avoid overheating of the sample, the required pulses can be issued in short "bursts", each followed by an idle interval for thermal reequilibration.

We point out that the hardware and software sketched above have been employed successfully in

other areas of research in magnetic resonance, such as ESR, ENDOR (both cw and pulsed) and NMR. Space does not allow to give further details, for which the authors should be contacted directly.

Results

Resonance Frequencies

The measured resonance frequencies of the four NQR lines are reported in Fig. 1 as functions of the temperature, which was varied between 77 K and 418 K, the latter being the temperature of incipient melting, as confirmed by direct visual observation of the sample through a hole in the brass shield. The reproducibility of resonance frequency measurements, either by NLLSQ or by the 3-point Gaussian procedure, was better than 50 Hz; therefore the slight dispersion of data was mainly the result of residual temperature fluctuations. The data at liquid He temperature, taken from literature [10], fit nicely the remaining ones, pointing out the usual flattening of the frequency/temperature curves at the lowest temperatures.

Line Widths and Amplitudes

At 77 K the signal to noise ratio (S/N) was in excess of 5 on a single FID. The FID could be detected on the scope up to the vicinity of the melting point. Its intensity was then considerably lower, but, because of the much shorter T_1 relaxation time, on long-term averaging the S/N was best, for a given accumulation time, a few degrees below the melting point. The results discussed in the following confirm more quantitatively this finding, indicating that the S/N should increase approximately as the absolute temperature T .

At all investigated temperatures the lines showed differences in amplitude and width. The two upper lines were consistently wider, and when a proper comparison was made, they also appeared to be of higher amplitude.

Due to the low asymmetry parameter, the lines of this sample may show a large Zeeman effect even with low magnetic fields. Therefore we used our Zeeman coil, powered by a very low current, to compensate the earth's magnetic field, which could have been responsible for the difference in width. The compensating field was calibrated, both in intensity and direction, by putting in place of the sample an air-driven turbine

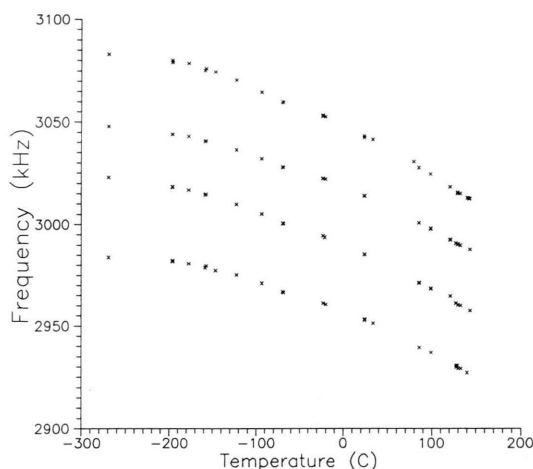


Fig. 1. Resonance frequency of ^{14}N lines of cyanuric chloride. The lines at 4.2 K are taken from [9]. The highest temperature is that of incipient melting of the sample.

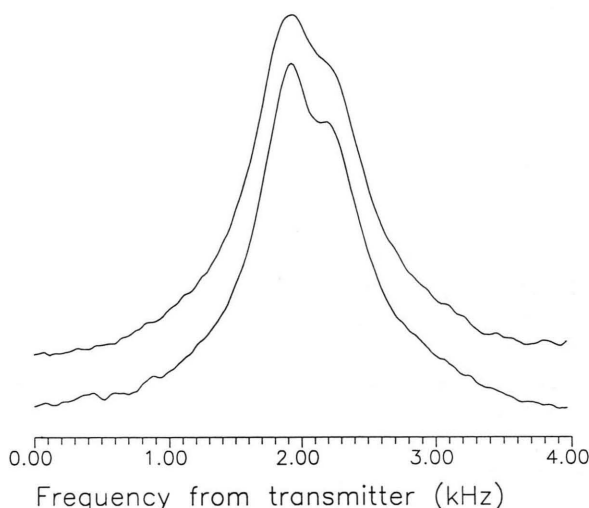


Fig. 2. NQR ^{14}N line of hexamethylenetetramine. Powder sample at room temperature. The modulus spectrum is shown as obtained in the earth's magnetic field (upper trace) and in zero magnetic field.

carrying a multiturn coil, which acted as a generator of measurable current in the presence of even a minute magnetic field. The effectiveness of the compensation was checked by recording the NQR line of hexamethylenetetramine at room temperature (Figure 2). The spectrum of cyanuric chloride, however, remained unchanged when compensation was employed (Fig. 3), demonstrating that the difference in line width is not an artifact due to Zeeman effect.

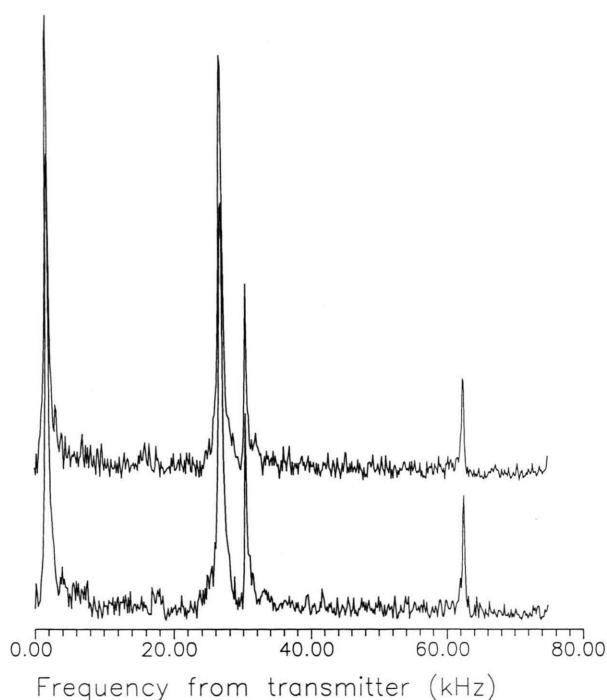


Fig. 3. NQR ^{14}N spectrum of cyanuric chloride. Experimental details as in Figure 2.

The spectrum of Fig. 3 was taken under typical measurement conditions, which included a maximum-response, 120° pulse [13] $40\ \mu\text{s}$ long and a high (about 120) Q merit factor for the coil. Both these conditions bring frequency selectivity which is quite significant over the spectral range studied, thus causing distortion of the amplitudes.

Figure 4 shows the full spectrum recorded at 77 K with a short pulse ($8\ \mu\text{s}$, or about 18°) and a resistor added in parallel to the sample coil in order to reduce its Q .

Although the sequence interval is lower than the measured T_1 , little saturation is present because of the short pulse length. This spectrum, which involves very little distortion of the amplitude ratios, still shows the two lower lines as being of lower amplitude than the upper ones.

Reliable values of the line widths could only be obtained by NLLSQ fitting of the spectra, the 3-point Gaussian being only suitable for yielding a starting value for subsequent fitting. The averaged line widths are reported (circles) in Fig. 5 as functions of temperature. The crosses in the same figure show the ratio of the average line widths of the two upper lines to that

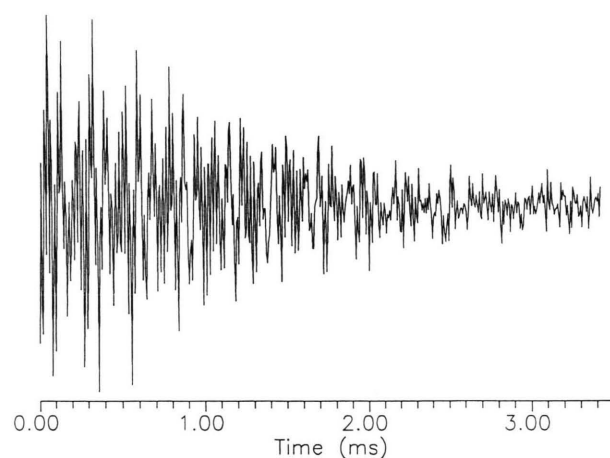
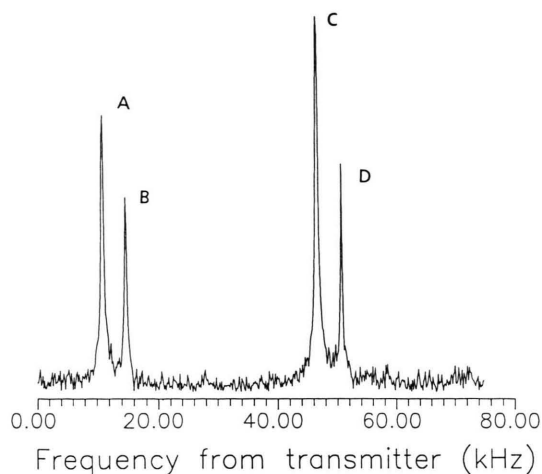


Fig. 4. ^{14}N NQR FID signal of cyanuric chloride (below) and its modulus spectrum at 77 K. Transmitter frequency is 3033 kHz. Pulse length and sample coil Q factor were reduced for wideband excitation and observation (see text). Lines B and D are below the transmitter frequency (see Table 1).

of the lower ones. The rationale for grouping and averaging the upper and lower lines is given in the Discussion section.

More complex procedures were necessary to be able to compare amplitudes from different spectra. We returned to high- Q conditions for maximum sensitivity, bringing each line of the spectrum in turn to appear in the 4 to 5 kHz range, where the selectivity of both excitation and sample circuit could be neglected. We also kept all other experimental conditions (amplifier gain, reference level, rf pulse height, etc.) as constant as we could. Finally, to be sure that saturation effects would be negligible, we took as line amplitude the

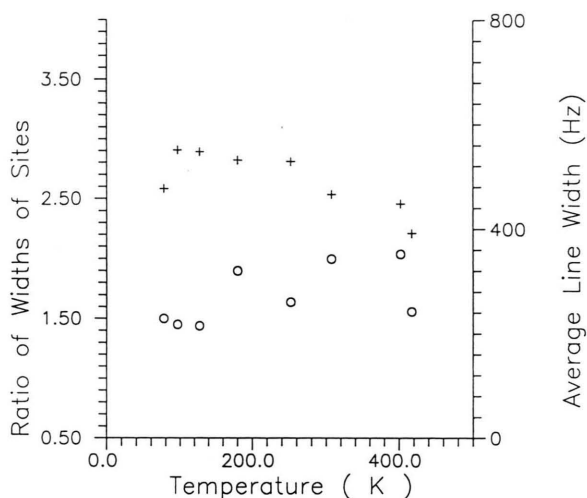


Fig. 5. Width of the ^{14}N NQR lines of cyanuric chloride as a function of temperature. Circles represent the ratio of the average width of the upper-frequency site to that of the lower-frequency one. Crosses represent the average width of the four lines.

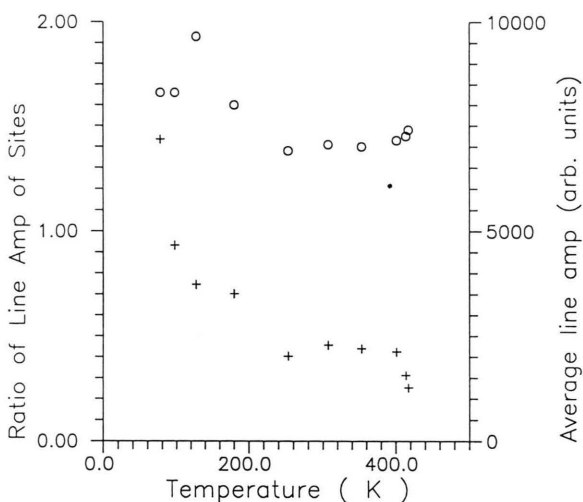


Fig. 6. Amplitude of the ^{14}N NQR lines of cyanuric chloride as a function of temperature. Circles represent the ratio of the average amplitudes of the upper-frequency site to that of the lower-frequency one. Crosses represent in arbitrary units the average amplitude of the four lines.

“infinity” value A_{inf} given by the NLLSQ fitting of data for T_1 measurement. The resulting amplitude values are reported in Fig. 6, with criteria similar to those of Fig. 5 for the line width.

T_1 Relaxation Time

Measurements were performed following the Progressive Saturation (PS) methodology. Given a start-

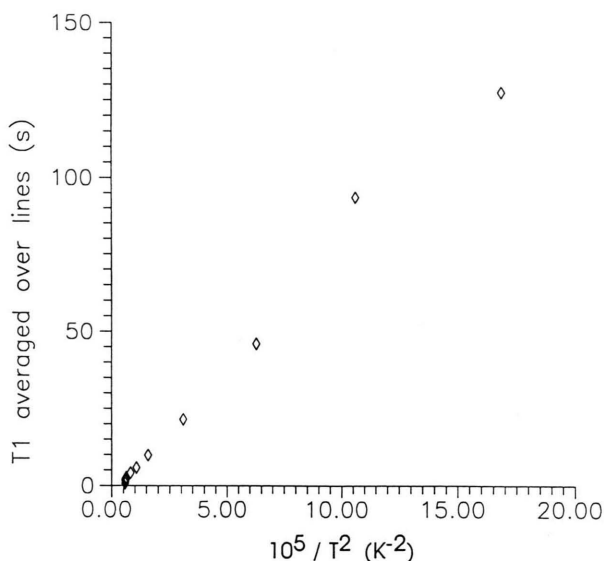
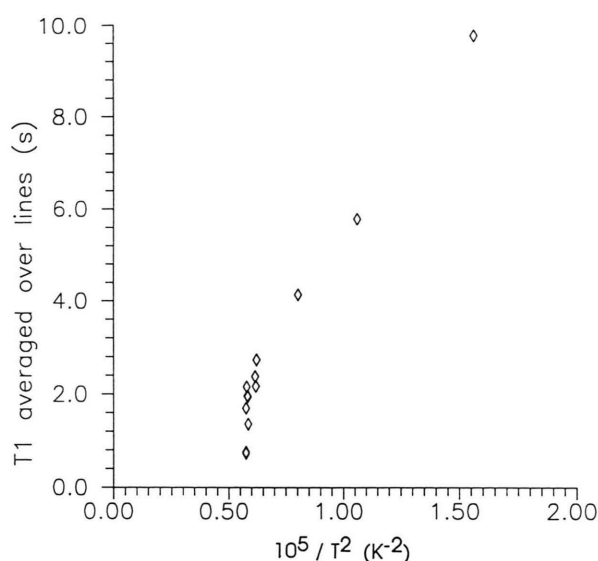


Fig. 7. T_1 relaxation time of cyanuric chloride as a function of the squared reciprocal of temperature. The average value of the four lines is shown. The full temperature range is shown below, while only the high-temperature values are reported in the expanded plot above. Note the precipitous behaviour on approach to the melting point.

ing estimate T_1' , the program automatically issues 7 acquisitions with as many different pulse separations t ranging from $t = 0.2 T_1'$ to $t = 2 T_1'$. The total acquisition time was kept constant for all t values, yielding an approximately constant S/N ratio. A sequence of 5 “idle” (no subsequent acquisition) pulses was inserted by the program, where necessary, to recover proper steady state of the magnetization.

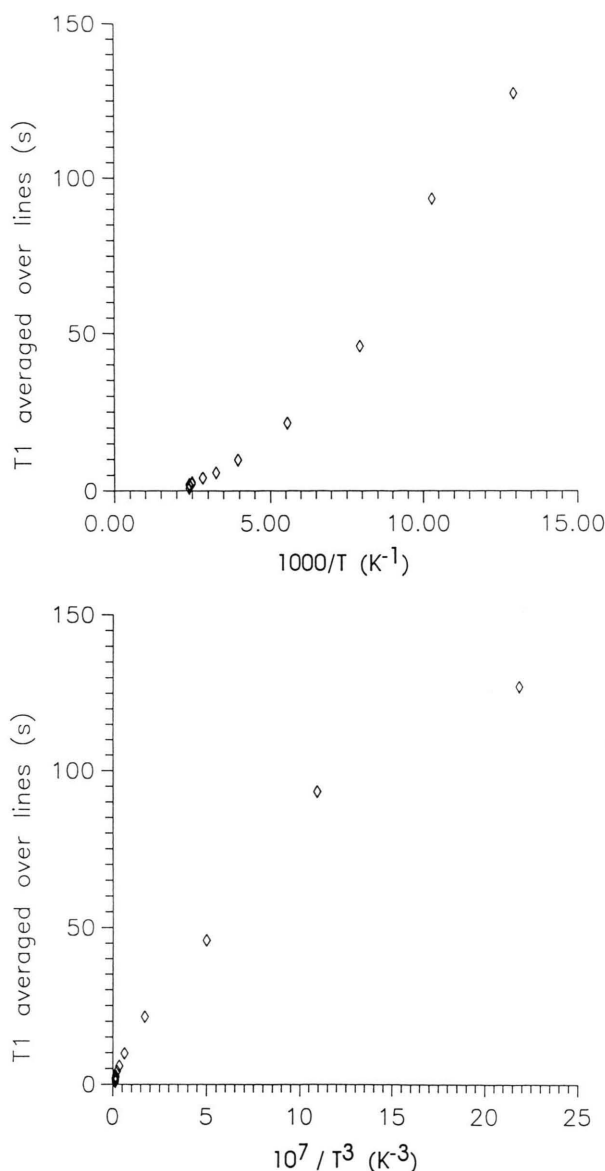


Fig. 8. T_1 relaxation time of cyanuric chloride as a function of the reciprocal of temperature (above) and of the cube of the reciprocal temperature (below). Comparison with the lower plot of Fig. 7 confirms the linear dependence of T_1^{-1} on the square of the absolute temperature.

The measured T_1 values are reported in Fig. 7 as a function of T^{-2} . The measured T_1 values spanned a wide range, from a maximum of 180 s at 77 K to slightly less than 1 s at the melting point. Since no significant difference between T_1 values for individual lines was found, except at the lowest temperature, their average value for each temperature is reported in

Table 1. Results of NLLSQ fitting of the data of Figure 6. The letters A, B, C, D refer to the corresponding lines in the figure. Resonance frequencies are measured with reference to the transmitter frequency. Standard deviations are given within parentheses.

NLLSQ fitting parameters for spectrum

Line	Type	Rel. amplitude	Width (Hz)	Resonance freq. (kHz)
A	ν_{up}^-	0.722 (0.009)	548 (11)	10.930 (0.004)
B	ν_{dn}^+	0.492 (0.008)	419 (3)	-14.640 (0.005)
C	ν_{up}^+	1.000 (0.009)	595 (8)	46.380 (0.003)
D	ν_{dn}^-	0.541 (0.011)	344 (10)	-50.514 (0.004)

NLLSQ fitting parameters for FID

Line	Type	Rel. amplitude	T_2^* (ms)	Resonance freq. (kHz)	Shape *
A	ν_{up}^-	0.68 (0.04)	1.8 (0.1)	10.840 (0.005)	1.8 (0.3)
B	ν_{dn}^+	0.35 (0.04)	2.3 (0.3)	-14.703 (0.007)	1.7 (0.5)
C	ν_{up}^+	1.00 (0.04)	1.7 (0.1)	46.280 (0.007)	1.8 (0.2)
D	ν_{dn}^-	0.29 (0.04)	2.8 (0.3)	-50.513 (0.008)	2.1 (0.7)

* The "shape" fitting parameters is 1 for a Lorentzian line, 2 for a Gaussian one. A Lorentzian line shape was used for best fit of the spectrum.

Figure 7. Also reported in the figure is an expanded plot of the high-temperature T_1 values against T^{-2} . The values of T_1 are also reported against T^{-1} and T^{-3} in Figure 8.

We attempted an NLLSQ fit of the data both in FID and FT modulus presentation. If the experimental parameters were such that the spectrum resulted to be effectively single-line, both methods yielded comparable results. When all four lines were of comparable amplitude, however, a fit of the modulus consistently yielded better results. In fact, standard deviations were lower (Table 1). The computation time was also reduced when the modulus was fitted. In the fact the fit was restricted to the points embracing 3 or 4 line widths when dealing with the modulus, and correspondingly to 3 or 4 times T_2^* when dealing with the FID. In practice this amounted, given the narrow lines of the present sample, to the inclusion of only a few tens of points in the fit of modulus. At least 500 points were needed for the fit of the FID, leaving small residual oscillations in the residuals, while residuals of the fit of the modulus were visually indistinguishable from random noise. All this is somewhat disappointing, since in principle the FID, which contains all available information and involves no phase error or other distortions, should be preferred for fit. In a sense

this richness of information could be the reason for the partial failure, since a phase (or acquisition delay) and a lineshape parameter also had to be included for convergence of the fit in the case of the FID.

Our estimate of the standard deviation on the measured quantities is the following: resonance frequency 30 Hz; line width 15 Hz; line amplitude 10%; T_1 15% to 20%; temperature 1 K; temperature stability within 0.25 K.

Discussion

Resonance Frequencies

The meaning of Fig. 1 is rather straightforward, although a bit surprising. First of all, the existence of four lines confirms the grouping of the three nitrogen atoms in the molecule in two nonequivalent sites, each yielding a ν^+ and a ν^- line. However, on the basis of frequency measurements alone, only the upmost and the lowest frequency lines can be safely identified as a ν^+ and a ν^- , respectively. The existence of two different sites in the molecule is confirmed by the two-line ^{35}Cl spectrum [2]. However, on the basis of the known X-ray structure [4] one could have expected that at some temperature there would have been a phase transition towards a rhombohedral structure conserving molecular symmetry, just as it happens for s-triazine [14] and presumably cyanuric fluoride [15]. In fact the monoclinic lattice still conserves elements related to ternary axes, such as the beta angle of nearly 60° [4] and the angles between the C–Cl bonds close to 120° [3]. As the approach to the symmetry of the free molecule would presumably involve the acquisition of rotational and/or translational freedom, corresponding effects on the relaxation times and/or appearance of a plastic transition could have been anticipated. This was the main reason for extending previous, partial studies [9] up to the melting point.

Nothing of the kind happens. A single phase is evidently stable over an exceptionally wide temperature range. Nor is there any hint of coalescence of the two sites to a single one. Instead, the already minute asymmetry parameter (η) tends to decrease even more. The average distance between the lines of the two sites remains approximately constant.

Line Amplitudes

A similar, strikingly uneventful behaviour is shown by most of the other NQR parameters. However, as

already noted, the two upper lines always have larger amplitude and width. The product of the factors for the ratio of the widths (Fig. 5) and of the amplitudes (Fig. 6) is at least 2 at all temperatures, and zero-field spectra (Fig. 3) show that the greater line width is not an artifact due to sample preparation. This is certain proof that the two upper lines pertain to the same site, as do the lower ones. Furthermore, the “upper” site appears to be the one corresponding to two chemically equivalent sites (for ^{35}Cl spectra the opposite is true [3 b]). This confirms and completes the previous assignment of lines to sites [10].

The average amplitudes are found to follow, within errors, a T^{-1} trend, indicating that the main reason for their temperature dependence is simply the Boltzmann factor for population of the quadrupolar states. Only at the melting point a faster decrease of amplitude was seen, which is probably the consequence of the partial transformation of the sample to the liquid state.

Line Widths

The line widths remain quite narrow up to the melting point, indicating the absence of any degree of temperature dependent disorder, despite the observation [3 b] of “paper pad” softness in cyanuric chloride crystals. Part of the slight line broadening at low temperature should be due to temperature instability, as in liquid nitrogen the line width decreases again (a rms temperature fluctuation of only 0.1 K could increase line width by about 10% through the temperature dependence of its resonance frequency).

The absolute values of the line width merit further comments. Taking into account the very low η of ^{14}N in cyanuric chloride, that makes two quadrupolar states quasi-degenerate, one expects incomplete quenching of the angular momentum of ^{14}N , hence a wide line in the presence of nuclei having a large magnetic moment. This happens for the analogous cyanuric fluoride [15] due to the strong dipole moment of the ^{19}F nuclei, and for HMT, where no quenching at all applies. In the present case of cyanuric chloride, however, the lines are quite narrow; this most probably stems from the absence of any nucleus having a large magnetic moment. One cannot push this argument too far. In fact we are assuming that the homogeneous contributions to the line width are important. It has been shown that the line broadening of s-triazine [14] is essentially inhomogeneous, so that a static magnetic

dipole should play a minor contribution to the line width. This seems to apply to cyanuric fluoride and chloride too, if one considers that echoes could be seen with large pulse separation [9, 14]. We may confirm this point for cyanuric chloride, although we failed to find proper (zero) response for "180°" pulses, probably due to insufficient homogeneity of the rf pulses over the sample, so that we cannot quote sufficiently reliable quantitative values.

T_1 Relaxation Time

The T_1 values are quite long at all temperatures, and essentially equal for the four lines within experimental error. Only below 130 K some significant difference between the T_1 values of the lines was found. The average values follow a smooth T^{-2} trend up to near the melting point (Figure 7). This trend is anticipated [16] for the basic, ever-present two-phonon Raman process. In contrast, in s-triazine both exponential dependence of T_1 on T and anisotropy of relaxation times have been found, the latter defined as difference between the transition probabilities associated with the different transitions. Anisotropy is quite difficult to detect, even in principle, in a system like cyanuric chloride, where essentially a single quadrupolar transition exists, due to the very small η . As far as the dependence on T is concerned, the fact that only an unspecific trend is found does not mean that special motional effects, such as molecular reorientation around the "quasi-ternary" axis, do not take place. Rather we would say that the coupling to such motions is too weak to give a measurable effect. This suggests that coupling to lattice modes should probably be through modulation of the magnetic dipole-dipole interaction. In fact, efg modulation is expected to be larger for cyanuric chloride than for s-triazine, due to the strong local dipoles present at the C–Cl bonds. Modulation of the efg should be even more effective in cyanuric fluoride, and probably is, given the very low T_1 and T_2^* values found for that sample [15]. The ratio of the factors for the effect of modulation of magnetic dipole interaction, based on known structure data in the gas phase for cyanuric chloride and fluoride [17, 18], would in fact account for only a factor of about 20, while the measured ratio for both relaxation times is greater than 100. However, although cyanuric fluoride is in principle attractive for such comparison, we must take into account that its low-temperature structure is certainly different from that of cyanuric chloride [15]. Furthermore, the very

broad, overlapping lines of cyanuric fluoride give rise to adverse measurement conditions, due to the impossibility to measure T_2^* directly and to the extreme difficulty of issuing a valid "90°" pulse for such a wide spectral coverage.

The "catastrophic" trend of T_1 towards the melting point (Fig. 7) is thus to be seen as the effect of rearrangement of phonon bands rather than as the direct coupling of new motional features to NQR transitions.

The low-temperature differentiation between the individual T_1 's of the four transitions becomes noticeable at 77 K, where the spread of the T_1 values is from 80 to 180 s, the low-frequency site having the shortest values. This could be due to the approach to the (unknown) Debye temperature of the crystal, which would introduce a different temperature dependence of T_1 and could give rise to a different effective phonon density as seen from the two sites. Although no T_1 measurement could have been performed at 4.2 K [10] due to the use of a continuous-wave Robinson spectrometer, it was found [19] that the lines of cyanuric chloride are less easily saturated than those of s-triazine, whose T_1 has been evaluated to be about 10 h [20]. Thus the T^{-2} trend, which a bold extrapolation would lead to about 48 h at 4.2 K, appears not to be followed below 77 K.

Electronic Structure

The singular electronic structure of cyanuric chloride is signaled by NQR especially through the value of the asymmetry parameter η , which is anomalously high (around 25%) for Cl, but anomalously low (around 1.5%) for N. We take 3,5-dichloropyridine [21] as a suitable reference compound, having both an aromatic nitrogen and chlorine as a ring substituent in the meta position, normally thought as being the least affected by modification of the aromatic structure. In such a compound the asymmetry parameter is 8.6% for Cl and 33% for N. The anomalous values found for cyanuric chloride can be qualitatively interpreted by standard chemical parametrization, which indicates Cl as an electron donor towards the aromatic system, pyridinic N as an electron acceptor. We also note that on going from pyridine [22] to 3,5-dichloropyridine, η of the N atom is little affected (from an average of 40% to 33%), while 2,6-dichloropyridine [21], whose substituted moiety is analogous to cyanuric chloride, has a low η for N (11%) and a moderately high one for Cl (12%) with respect to the chosen reference. Never-

theless, the entity of the further difference between 2,6-dichloropyridine and cyanuric chloride is outstanding. Previous analyses of the electronic structure of cyanuric chloride in relation to NQR results and the related theoretical calculations [23] described this molecule as having a particularly high electron mobility in relation to ring substitution. More recent X-ray work [24], while unfortunately not reporting structure data, gives an accurate map of the differential electronic density of the cyanuric chloride molecule with respect to the component atoms. Extended delocalization of π orbitals and deformation of the Cl and N lone pairs are evident and could not be reproduced satisfactorily even by SCF molecular orbital calculations on extended bases [24]. In view of this, the application of "theories", such as the Townes-Dailey approximation, based on consideration of valence atomic orbitals in the molecule, appears futile and may even be misleading. Doing so [15] one obtains, for instance, a larger π donation from F than from Cl, which is clearly contrary to chemical intuition.

However, NQR is still useful in indicating that the origin of the "anomalous" η values in this "hyperaromatic" compound has to be found in intramolecular effects. In fact, the differential solid-state effect between the two sites, as measured by the average frequency difference between them, is very small, comparable to the effect of the minute value of η . ^{35}Cl NQR also indicates small solid-state effects. The values of η for both sites are essentially the same. Furthermore, this situation is maintained over an extended range of temperature, up to the limit of stability of the

solid phase. Finally, Zeeman NQR results point out an essentially planar ring structure [3]. Overall, this strongly suggests that further analysis of the electronic structure of the isolated molecule would be a worthy effort for the explanation of NQR data.

Conclusion

The instrumental innovations introduced in our NQR apparatus have allowed to perform correctly measurements which from many points of view appeared to be challenging. The analysis of the data led to a significant increase of the knowledge on cyanuric chloride, of its peculiar electronic structure and of some static and dynamic aspects of its state in the crystal. As it frequently happens, the results obtained suggest to perform further work, in particular extended calculations on the electronic structure and ^{14}N Zeeman measurements on a single crystal, the latter being able, among other things, to yield reliable information on the direction of the efg axes at N. We hope to be able to perform both tasks in the near future.

Acknowledgements

We wish to thank Mr. Agile Papini for technical assistance in the modification of the data-acquisition interface and Mr. Andrea Biagi for working out some of the high-level code. We also gratefully acknowledge the referee for his very careful reading of the manuscript and the ensuing suggestions.

- [1] D. G. Neilson and D. Hunter, in: *Rodd's Chemistry of Carbon Compounds* (M. F. Ansell, ed.), vol. IV^U, p. 474, Elsevier, Amsterdam 1989.
- [2] H. Negita and S. Satou, *J. Chem. Phys.* **27**, 602 (1957).
- [3] a) Y. Morino, T. Chiba, T. Shimozaawa, and M. Toyama, *J. Phys. Soc. Japan* **13**, 869 (1958). – b) F. J. Adrian, *J. Chem. Phys.* **19**, 1381 (1958).
- [4] W. Hoppe, H. U. Lenné, and G. Morandi, *Z. Kryst.* **108**, 321 (1957).
- [5] Y. Morino and M. Toyama, *J. Chem. Phys.* **35**, 1289 (1961).
- [6] S. Kojima and M. Minematsu, *J. Phys. Soc. Japan* **15**, 355 (1960).
- [7] R. Lenk and E. A. C. Lucken, *Pure Appl. Chem.* **40**, 199 (1974).
- [8] R. Ramachandran and E. Oldfield, *J. Chem. Phys.* **80**, 674 (1984).
- [9] C. Stutz and D. Early, *J. Mol. Struct.* **111**, 31 (1983).
- [10] A. Péneau, B. Manallah, and L. Guibé, *Z. Naturforsch.* **41a**, 192 (1986).
- [11] R. Ambrosetti and D. Ricci, *Rev. Sci. Instrum.* **62**, 2281 (1991).
- [12] A. Colligiani and R. Ambrosetti, *Gazz. Chim. It.* **106**, 439 (1976).
- [13] S. Vega, *J. Chem. Phys.* **61**, 1093 (1974).
- [14] A. Zussman and M. Oron, *J. Chem. Phys.* **66**, 743 (1977).
- [15] C. Stutz, K. Garcia, and S. Cochran, *Z. Naturforsch.* **41a**, 399 (1986).
- [16] A. Abragam, *The Principles of Nuclear Magnetism*, p. 406, Oxford, London 1961.
- [17] Y. Akimoto, *Bull. Chem. Soc. Japan* **28**, 1 (1955).
- [18] S. H. Bauer, K. Katada, and K. Kimura, in: *Structural Chemistry and Molecular Biology* (A. Rich and N. Davidson, eds.), p. 653, W. M. Freeman & Co., San Francisco 1968.
- [19] L. Guibé, private communication.
- [20] B. Manallah, *Z. Naturforsch.* **41a**, 396 (1986).
- [21] R. Ambrosetti, R. Angelone, and A. Colligiani, *J. Mol. Struct.* **58**, 171 (1980).
- [22] L. Guibé, *C. R. Acad. Sci.* **250**, 3014 (1960).
- [23] Y. E. Shaposhnikov, Y. B. Yasman, T. G. Sukhanova, and V. A. Danilov, *Org. React. (Tartu)* **21**, 441 (1984).
- [24] Z. Darakjian, W. H. Fink, and H. Hope, *J. Mol. Struct.* **202**, 111 (1989).